



Article

Chemical Constituents, Quantitative Analysis, Anti-SARS-CoV-2 and Antioxidant Activities of Herbal Formula “Ping An Fang Yu Yin”

Yun-Chen Tsai ¹, Ming-Chung Lee ², Yu-Hui Hsieh ³, Kun-Teng Wang ⁴, Chao-Yu Chen ⁴, Wu-Chang Chuang ^{1,*} and Jih-Jung Chen ^{5,6,*}

¹ Sun Ten Pharmaceutical Co., Ltd., New Taipei City 231030, Taiwan

² Brion Research Institute of Taiwan, New Taipei City 231030, Taiwan

³ Biomedical Industry Ph.D. Program, School of Life Sciences, National Yang Ming Chiao Tung University, Taipei 112304, Taiwan

⁴ Herbiotek Co., Ltd., New Taipei City 231030, Taiwan

⁵ Department of Pharmacy, School of Pharmaceutical Sciences, National Yang Ming Chiao Tung University, Taipei 112304, Taiwan

⁶ Department of Medical Research, China Medical University Hospital, China Medical University, Taichung 404332, Taiwan

* Correspondence: cwctd331@sunten.com.tw (W.-C.C.); jjungchen@nycu.edu.tw (J.-J.C.); Tel.: +886-2-2826-7195 (J.-J.C.)



Citation: Tsai, Y.-C.; Lee, M.-C.; Hsieh, Y.-H.; Wang, K.-T.; Chen, C.-Y.; Chuang, W.-C.; Chen, J.-J. Chemical Constituents, Quantitative Analysis, Anti-SARS-CoV-2 and Antioxidant Activities of Herbal Formula “Ping An Fang Yu Yin”. *Processes* **2022**, *10*, 2213. <https://doi.org/10.3390/pr10112213>

Academic Editors: Kelvin Chan, Karl Tsim and Yingqing Du

Received: 17 September 2022

Accepted: 24 October 2022

Published: 27 October 2022

Publisher’s Note: MDPI stays neutral with regard to jurisdictional claims in published maps and institutional affiliations.



Copyright: © 2022 by the authors. Licensee MDPI, Basel, Switzerland. This article is an open access article distributed under the terms and conditions of the Creative Commons Attribution (CC BY) license (<https://creativecommons.org/licenses/by/4.0/>).

Abstract: COVID-19 is a global pandemic infectious disease caused by severe acute respiratory syndrome coronavirus 2 (SARS-CoV-2). The herbal formula, Ping An Fang Yu Yin (PAFYI), has been used to prevent respiratory viral infections for many years. This study aims to evaluate the effect of PAFYI on SARS-CoV-2 infection, oxidative stress, and inflammation via in vitro, investigate the chemical composition by full constituent quantitative analysis, and verify its anti-viral potential against SARS-CoV-2 using in silico. In this study, a total of eleven compounds, twenty amino acids, saccharide compositions, and trace elements were found and quantitatively determined by chromatographic techniques. PAFYI displayed free radical scavenging activity (DPPH, SC_{50} : 1.24 ± 0.09 mg/mL), SOD activity ($68.71 \pm 1.28\%$), inhibition of lipoxygenase activity (75.96 ± 7.64 mg/mL) and interfered the interaction of SARS-CoV-2 spike protein and angiotensin-converting enzyme 2 ($48.04 \pm 3.18\%$). Furthermore, in-silico analysis results supported that liquiritin, 3,5-dicaffeoylquinic acid, and luteolin-7-O-glucoside with the highest affinity between SARS-CoV-2 RBD and human angiotensin-converting enzyme II (hACE2) receptor. Our findings suggest that PAFYI has the potential for anti-SARS-CoV-2 infection, anti-oxidation stress, and anti-inflammation, and may be used as supplements for amelioration or prevention of COVID-19 symptoms, as well as the representative compounds can be used for quality control of PAFYI in the future.

Keywords: Ping An Fang Yu Yin; anti-SARS-CoV-2; antioxidant; chromatographic techniques; fingerprints analysis

1. Introduction

COVID-19 is a severe acute respiratory syndrome caused by the coronavirus (SARS-CoV-2), which has become a global pandemic since 2019. More than 603 million confirmed cases and 6.48 million deaths had been reported to WHO by 7 September 2022 [1]. The most common symptoms are asymptomatic/mild-to-moderate respiratory disease, which in patients can become life-threatening conditions such as severe pneumonia and acute respiratory distress syndrome (ARDS) [2,3]. The spike protein is a crucial factor in the SARS-CoV-2 infected host cell. When the virus attaches to the host cell, the spike protein interacts with angiotensin-converting enzyme 2 (ACE2), causing the virus to infect the host cell [4]. In addition, recent reports suggest that inflammation and oxidative stress are important in

the transition from mild to severe symptoms in COVID-19 patients, increasing the risk of organ damage and complications [5,6]. Anti-inflammatory agents, 5-lipoxygenase (5-LOX) inhibitors, can reduce SARS-CoV-2-mediated inflammatory diseases, including cytokine release syndrome and ARDS during reprogrammed immune cells and mediators [7]. In addition, antioxidants can reduce the risk of complications and attenuate the prognosis in COVID-19 cases by scavenging reactive oxygen species and oxidant-producing enzymes [8]. Therefore, supplementation with antioxidant, anti-inflammatory, and anti-SARS-CoV-2 agents may contribute to the prevention and treatment of COVID-19.

Traditional Chinese medicine (TCM) is the oldest, most unique, and complete medical system. TCM has the characteristics of multi-component and multi-target in the prevention and treatment of diseases. It also showed positive efficacy and tolerable toxicity. Shang Han Lun, Wen Yi Lun, and Jheng Jih Huei Bu were the famous ancient TCM book about the systematic study of internal medicine, such as infectious disease, and as the reference book for infection diseases until now. Pharmacological studies have displayed that TCM formulas have multiple efficacies in COVID-19 treatment, including “RespireAid (NRICM101)” and “Jing Guan Fang” [9–12].

Ping An Fang Yu Yin (PAFY) is a Chinese herbal formula that has been used to prevent respiratory viral infections for years. PAFY is a reference to the ancient TCM book and modified from Huang Qi Ge Gen Tang and Gan Ju Tang. The formula was composed of Houttuynia, Pueraria, Astragalus, Honeysuckle flower, Citrus peel, Agastache, Licorice, Mentha, Codonopsis, Platycodon, and Perilla leaf. Previous research exhibited that Houttuynia, Astragalus, Licorice, Honeysuckle flower, Platycodon, Mentha, Pogostemon, and Perilla leaf can anti-SARS-CoV-2 invasion and replication activities. The Citrus peel, Houttuynia, Pueraria, Astragalus, Honeysuckle flower, Pogostemon, Licorice, Mentha, Codonopsis, Platycodon, and Perilla leaf have antioxidative and anti-inflammatory activities [13–20]. The puerarin, rosmarinic acid, hesperidin, chlorogenic acid, and glycyrrhizic acid have an anti-SARS-CoV-2 effect by interfering with the ACE2 receptor and SARS-CoV-2 spike protein interaction [14–16,21]. The bioactivity of traditional Chinese herbal formulas is not derived from a single compound but from the interaction of many active components. However, the anti-viral infection principles of PAFY and its chemical composition have never been described.

The chemical composition of PAFY is very complex. Therefore, it seems feasible to use multiple fingerprint techniques to assess the quality of PAFY [22]. The aim of this study is to identify and quantify various chemical constituents in PAFY and investigate the antioxidative, anti-inflammatory, and anti-SARS-CoV-2 activities of PAFY, as well as related to COVID-19 to know its preventative potential by *in vitro* and *in silico* studies.

2. Materials and Methods

2.1. Material and Reagent

The acetonitrile (ACN) and methanol were purchased from Honeywell (Charlotte, NC, USA). The water was purified by a Thermo water purification system (Thermo Fisher Scientific, Waltham, MA, USA). Potassium dihydrogen phosphate and phosphoric acid were purchased from Merck (Darmstadt, Germany). Reference materials for polysaccharides, stachyose, D-(–)-fructose, D-(+)-glucose, sucrose, and L-amino acids kit (LAA21) were purchased from Sigma-Aldrich (USA). Ping An Fang Yu Yin (PAFY, All Mighta Plus), Houttuynia, Pueraria, Astragalus, Honeysuckle flower, Citrus peel, Agastache, Licorice, Mentha, Codonopsis, Platycodon, and Perilla leaf were manufactured by Sun Ten Pharmaceutical company (New Taipei City, Taiwan). The preparation method of PAFY tea was described in the Supplementary Materials.

2.2. Fingerprints Analysis in PAFY

Preparation of PAFY standard solution, 0.5 g of PAFY and its individual herbs were extracted with 70% methanol (20 mL), and the solution was sonicated at 25 °C for 15 min, then shaken at 160 rpm in a 40 °C water bath at 20 min. Accurately weigh appro-

appropriate amounts of quercitrin, rosmarinic acid, hesperidin, chlorogenic acid (Sigma-Aldrich, St. Louis, MO, USA), calycosin-7-O-glucoside, liquiritin (PhytoLab, Vestenbergsgreuth, Germany), 3,5-dicaffeoylquinic acid, lobetyolin, platycodin D (SunHank, Tainan, Taiwan), astragaloside IV, puerarin (National Institutes for Food and Drug Control, Beijing, China), glycyrrhizic acid (Taiwan Food and Drug Administration, Taipei, Taiwan), luteolin-7-O-glucoside (Fusol Material, Tainan, Taiwan) were added in a volumetric flask, 70% methanol was added as a diluent, and sonicated at 25 °C for 15 min. All the samples were filtered by a 0.45 µm filter, and the solution was further assayed for small organic molecules.

The HPLC/PDA analytical system used Waters 600 and 2996 instruments (Waters, Milford, MA, USA). The conditions of analysis were controlled as follows: gradient elution through mobile phase A (1 L of 20 mM KH₂PO₄ with 0.01% H₃PO₄), B (ACN), and C (H₂O) at 0–30 min with the ratio of 90–75% A and 10–25% B; at 30–40 min, a ratio of 75–65% A and 25–35% B; at 40–55 min, a ratio of 65–0% A, 35–75% B, and 0–25% C; at 55–60 min 75–10% B and 25–90% C; and at 60–65 min with 0–90% A, 10% B, and 90–0% C. The rate of flow was 1.0 mL/min (running time: 65 min). The 200–400 nm was set to detection. Cosmosil 5C₁₈-MS-II column (5 µm, 4.6 × 250 mm, Nacal tesque, Kyoto, Japan) was used as an analytical column. The guard column was a Lichrospher RP-18 capped column (5 µm, 4.6 × 10 mm, Merck, Darmstadt, Germany).

The fingerprint analyses of saccharides, amino acids, and trace elements is described in the supplementary information.

2.3. Bioactivity Assay

Extract about 1 g of sample powder with water (10 mL). Sonicate the solution at 25 °C for 20 min, then shake at 160 rpm for 20 min in a water bath (40 °C). All the samples were filtered by a 0.45 µm filter.

The free radical scavenging activity of 200 µM DPPH (1,1-diphenyl-2-picrylhydrazyl): Mix 100 µL sample solution with 100 µL DPPH ethanolic solution (Cat Nr: D4313, TCI America, Portland, OR, USA). The mixture was incubated at room temperature for 30 min. A517 nm was measured using the SPECTROstar Nano microplate reader (BMG Labtech, Ortenberg, Germany). DPPH scavenging effect was calculated by the following expression.

$$\text{Scavenging activity \%} = (1 - \text{Absorbance of sample} - \text{blank} / \text{Absorbance of control} - \text{blank}) \times 100$$

Nitric oxide radical scavenging assay: The sample solution (80 µL) combines with 20 µL of 25 mM sodium nitroprusside (Cat Nr: PHR1423, Sigma-Aldrich, St. Louis, MO, USA). After 2 h, the incubation solution was mixed with 100 µL Griess reagent (Cat Nr: G4410, Sigma-Aldrich, St. Louis, MO, USA). We measured the absorbance (540 nm) using the SPECTROstar Nano microplate reader (BMG Labtech, Ortenberg, Germany). The nitric oxide radical scavenging effect was calculated by the following expression:

$$\text{Scavenging activity \%} = (1 - \text{Absorbance of sample} - \text{blank} / \text{Absorbance of control} - \text{blank}) \times 100$$

The sample solutions were measured for superoxide dismutase activity (Cat Nr: CS0009, Sigma-Aldrich, St. Louis, MO, USA), lipoxygenase inhibition (Cat Nr: 760700, Cayman Chemical Company, Ann Arbor, MI, USA), and inhibition of SARS-CoV-2 spike interaction with ACE2 (Cat Nr: 502050, Cayman Chemical Company, Ann Arbor, MI, USA) on the basis of the manufacturer's instructions. Data are expressed as mean ± SD (*n* = 3). Statistical analysis was executed using the student's *t*-test (*p*-value < 0.05 was considered statistically significant).

2.4. Molecular Modeling Docking Study

The *in silico* evaluation was performed with AutoDock Vina (ADT ver. 4.0.1) (Scripps Research, San Diego, CA, USA) software [23]. Crystal structures of the SARS-CoV-2 spike protein receptor-binding domain (RBD) and human ACE2 (hACE2) complex (PDB: 6M17) were retrieved from the Protein Data Bank, and hydrogen atoms were added to prepare the docked receptors. The 3D structures of the ligands were constructed in the

Chem3D program Ultra 12.0 (PerkinElmer, Cambridge, MA, USA). The Gasteiger charge measurement of the protein atoms and the selection of the flexible twist of the ligand was performed by AutodockTools (ADT ver. 1.5.6) (Scripps Research, San Diego, CA, USA). The binding affinity energy is provided as a docking fraction and measured in kcal/mol. The visualization of the best docking interactions was analyzed in Biovia Discovery Studio Client 2021 (DS Biovia, San Diego, CA, USA) [24].

3. Results

3.1. Determination of Multiple Chemical Ingredients

The quercitrin, rosmarinic acid, hesperidin, chlorogenic acid, calycosin-7-*O*-glucoside, liquiritin, 3,5-dicaffeoylquinic acid, lobetyolin, platycodin D, astragaloside IV, puerarin, glycyrrhizic acid, and luteolin-7-*O*-glucoside were used as reference standards (Figure 1) and then analyzed which herbal material relates to the chromatographic peak of PAFYY by using HPLC/PDA or ELSD detection. By comparison with the standard reference compounds, eleven compounds were identified, including quercitrin, rosmarinic acid, hesperidin, chlorogenic acid, liquiritin, 3,5-dicaffeoylquinic acid, lobetyolin, astragaloside IV, puerarin, glycyrrhizic acid and luteolin-7-*O*-glucoside (Figure 2 and Supplementary Figure S1). The concentration of compounds is shown in Table 1. Puerarin, chlorogenic acid, hesperidin, glycyrrhizic acid, and liquiritin were the main compositions (≥ 1 mg/g) of PAFYY. The possible effect of these compounds was described in the discussion section.

The fingerprints of carbohydrates, amino acids, and trace elements in PAFYY are shown in Supplementary information. Based on the data, the polysaccharide was determined to be 13.12 mg/g and calculated as glucose according to the HPLC/RI method (Figure S2). PAFYY was rich in amino acids, especially essential amino acids. Proline was found to be the most abundant free form of amino acid. Branched-chain amino acids such as Leucine were found to be the most abundant amino acid in their hydrolyzed form by LC-MS/MS method (Table S1). Major trace elements found in PAFYY, including Mg, K, and Ca, by ICP/MS analysis (Table S2).

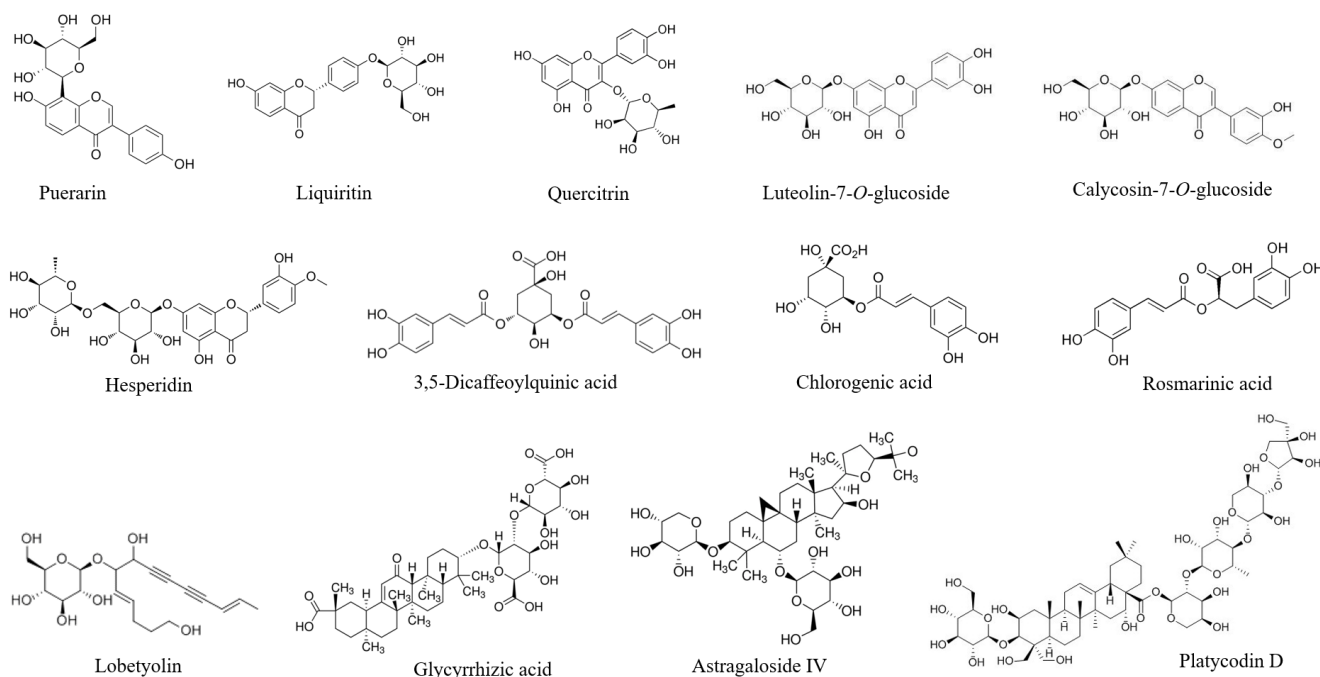


Figure 1. Chemical structure of the active ingredients of the PAFYY.

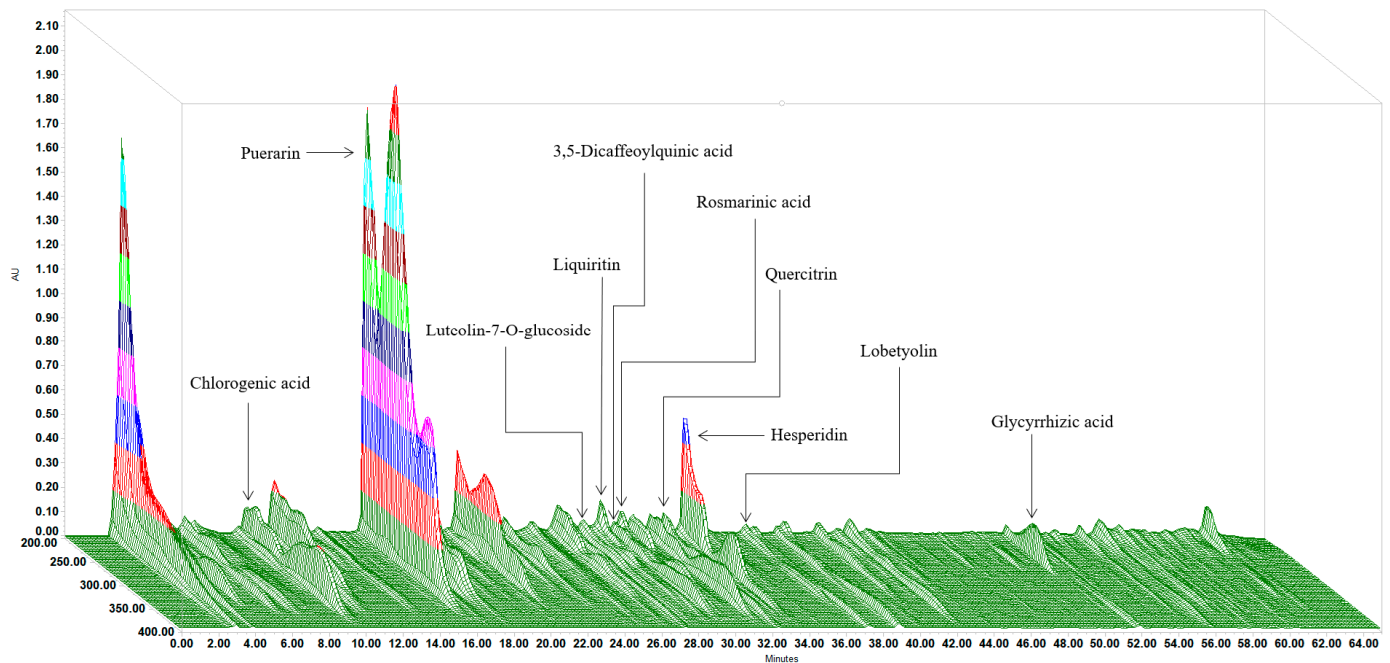


Figure 2. Chromatographic fingerprints of PAFYY from 3D-HPLC/PDA.

Table 1. Herbal content and retention time of 11 components in PAFYY.

Herbal Material in PAFYY	Reference Substance	Retention Time (min)	Content (mg/g)
Astragalus	Astragaloside IV	32.00	0.12
Astragalus	Calycosin-7-O-glucoside	25.49	BQL
Houttuynia	Quercitrin	32.64	0.50
Houttuynia, Honeysuckle flower	Chlorogenic acid	9.96	2.98
Honeysuckle flower	3,5-Dicaffeoylquinic acid	29.77	0.55
Honeysuckle flower	Luteolin-7-O-glucoside	28.45	0.10
Citrus Peel	Hesperidin	33.70	2.49
Codonopsis	Lobetyolin,	36.04	0.16
Licorice	Glycyrrhizic acid	51.02	2.00
Licorice	Liquiritin	26.85	1.12
Mentha, Perilla leaf	Rosmarinic acid	30.13	0.27
Platycodon	Platycodin D	23.5	BQL
Pueraria	Puerarin	16.39	10.90

BQL: below quantitation limit.

3.2. Anti-Oxidant Activity of PAFYY and Herbs Extraction

Due to the complexity of phytochemicals, two or more different *in vitro* assays may be used to evaluate herbal products. These tests are based on distinctive characteristics of antioxidative activity, including the ability to scavenge free radicals or SOD enzyme activity. Citrus peel and Honeysuckle flower exhibited antioxidative activity and a positive control for scavenging free radicals and SOD enzyme, respectively [25,26].

As shown in Figure 3A, PAFYY showed the inhibitory effect of DPPH free radicals (SC_{50} , 1.24 ± 0.09 mg/mL). The water extracts of individual herbs exhibited DPPH scavenging activity (Table 2). In addition, Houttuynia (1.72 ± 0.18 mg/mL), Pueraria (1.07 ± 0.08 mg/mL), Honeysuckle flower (0.58 ± 0.04 mg/mL), Mentha (0.25 ± 0.00 mg/mL), Licorice (2.09 ± 0.17 mg/mL) and Perilla leaf (0.53 ± 0.05 mg/mL) displayed higher DPPH scavenging activity than the positive control, which may be related to DPPH scavenging activity of PAFYY.

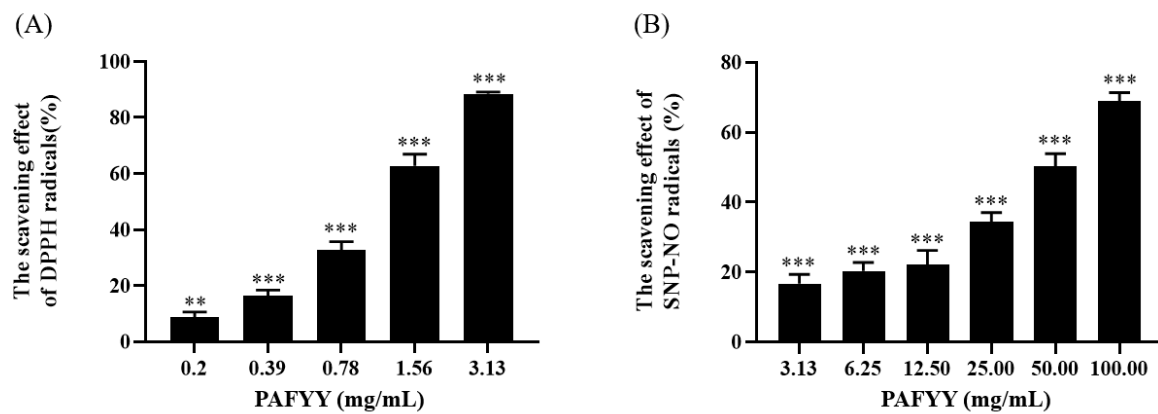


Figure 3. Antioxidant activity as measured by DPPH (A) and SNP-NO (B) assays as described for PAFYY. Asterisks show significant differences compared to control based on one-way ANOVA with Dunnett's multiple comparison test (** $p < 0.01$ and *** $p < 0.001$).

Table 2. Antioxidative activity of aqueous extract solutions of PAFYY and individual herbs measured by DPPH and SNP-NO scavenging assays.

Herbs	SC ₅₀ (mg/mL) ^a	
	DPPH Scavenging Assay	SNP-NO Scavenging Assay
Houttuynia	1.72 ± 0.18 ***	70.80 ± 2.19
Pueraria	1.07 ± 0.08 ***	25.99 ± 2.54 ***
Astragalus	24.44 ± 1.34	>100
Honeysuckle flower	0.58 ± 0.04 ***	25.01 ± 4.07 ***
Agastache	3.74 ± 0.62	62.26 ± 15.96
Mentha	0.25 ± 0.00 ***	19.62 ± 1.65 ***
Codonopsis	11.52 ± 1.85	>100
Licorice	2.09 ± 0.17 ***	>100
Platycodon	6.89 ± 1.03	>100
Perilla leaf	0.53 ± 0.05 **	12.11 ± 0.46 ***
Citrus peel ^b	3.96 ± 0.11	75.60 ± 3.10
PAFY	1.24 ± 0.09 ***	48.93 ± 4.96 **

^a SC₅₀ value is defined as half of the maximum inhibitory concentration. ^b The positive control was Citrus peel. Asterisks indicates significant difference between positive control herb based on *t*-test (** $p < 0.01$ and *** $p < 0.001$).

The inhibition of nitric oxide radicals is shown in Figure 3B. The results showed that PAFYY scavenged nitric oxide free radicals (SC₅₀: 48.93 ± 4.96 mg/mL). As for the individual water extracts determined in the experiments (Table 2). Pueraria (25.99 ± 2.54 mg/mL), Honeysuckle flower (25.01 ± 4.07 mg/mL), Mentha (19.62 ± 1.65 mg/mL), and Perilla leaf (12.11 ± 0.46 mg/mL) presented higher NO scavenging activity than that of positive control, which may relate to the NO scavenging activity of PAFYY.

In Table 3, PAFYY showed significantly higher superoxidase dismutase activity compared to the control group. We further analyzed water extracts of the herbs in the experiments, as shown in Table 4. The SOD activity of Houttuynia, Astragalus, Citrus Peel, Agastache, and Platycodon were higher than the positive control, which may be related to the SOD activity of PAFYY. As mentioned above, these results suggest that PAFYY may be used as an antioxidant.

Table 3. Effect of PAFYY tea (100 mg/mL) on SOD, LOX, and SARS-CoV-2 spike with ACE2 interaction.

	Inhibition Rate (%)		
	SOD Activity (%)	LOX Inhibition Rate (%)	Interaction of SARS-CoV-2 Spike with ACE2 Activity (%)
PAFYF	68.71 ± 1.28 ***	75.96 ± 7.64 ***	48.04 ± 3.18 ***

Asterisks (***) $p < 0.001$ indicate significant differences compared to *t*-test based controls. Data are presented as mean ± SD, $n = 3$.

Table 4. Effect of herbal aqueous extract on SOD, LOX, and SARS-CoV-2 spike with ACE2 interaction.

Herbs	SOD Activity (Unit/mL) ^a	LOX IC ₅₀ (mg/mL) ^b	SARS-CoV-2 Spike with ACE2 Interaction Activity IC ₅₀ (mg/mL) ^b
Houttuynia	14.89 ± 1.56 ***	2.31 ± 0.14 **	22.08 ± 3.70 ***
Pueraria ^d	3.82 ± 0.16	>100	91.69 ± 7.44
Astragalus	12.90 ± 1.93 **	40.75 ± 21.15	>100
Citrus peel	8.43 ± 0.18 **	>100	>100
Agastache	12.91 ± 1.76 **	>100	>100
Mentha	4.21 ± 0.26	3.70 ± 0.52 **	12.33 ± 2.13 ***
Codonopsis	5.68 ± 0.25	>100	11.29 ± 2.09 ***
Licorice	1.72 ± 0.17	>100	55.53 ± 4.00
Platycodon	17.29 ± 2.70 **	31.16 ± 2.37	19.85 ± 2.72 ***
Perilla leaf	3.20 ± 0.04	>100	13.02 ± 1.50 ***
Honeysuckle flower ^c	6.79 ± 0.23	13.83 ± 3.60	55.21 ± 31.97

^a Each herb was tested at 100 mg/mL. ^b The value of IC₅₀ was defined as half-maximal inhibitory concentration.

^c Honeysuckle as a positive control for SOD and LOX assays. ^d Pueraria as a positive control for the SARS-CoV-2 spike-ACE2 interaction assay. Asterisks indicate significant differences between positive control herbs based on *t*-test (** $p < 0.01$ and *** $p < 0.001$).

3.3. Anti-LOX Activity of PAFYY and Herbs Extraction

The PAFYY and herbal materials evaluated for the 15-LOX inhibitory activity. Honeysuckle flower showed anti-inflammatory activity and served as a positive control [26]. PAFYY was able to inhibit 75.96 ± 7.64% of 15-LOX activity at 100 mg/mL (Table 3). In Table 4, Houttuynia, Astragalus, Mentha, Platycodon, and Honeysuckle flower could inhibit the activity of 15-LOX to varying degrees. The dose-response analysis showed that the half-maximal inhibitory concentration of Houttuynia, Mentha, and Honeysuckle flower on 15-LOX were 2.31 ± 0.14, 3.7 ± 0.52 and 13.83 ± 3.6 mg/mL, respectively. These results suggest that PAFYY may regulate the LOX by Houttuynia, Mentha, and Honeysuckle flowers.

3.4. Effect of PAFYY and Herbs Extraction on SARS-CoV-2 Spike with ACE2 Interaction

PAFYF suppressed the SARS-CoV-2 spike with ACE2 interaction, and the inhibition rate was 48.04 ± 3.18 mg/mL (Table 3). In Table 4, Houttuynia, Honeysuckle flower, Mentha, Codonopsis, Licorice, Platycodon, Perilla leaf, and Pueraria inhibited the interaction of SARS-CoV-2 spike with ACE2 (IC₅₀: 11.29 to 91.69 mg/mL). These results indicate that PAFYY can be used as an anti-SARS-CoV-2 agent. Houttuynia, Mentha, Codonopsis, Platycodon, and Perilla leaf may play important roles in the anti-SARS-CoV-2 activity of PAFYY.

3.5. Molecular Modeling Docking Study

To further investigate the interaction between bioactive compounds and SARS-CoV-2 spike protein with the cellular receptor ACE2 and try to explain how these compounds exert their antagonistic effects, docking models of compounds were generated using Discovery Studio 2021 (Accelrys, San Diego, CA, USA) modeling program. The crystal structure (PDB: 6M17) of SARS-CoV-2 spike protein RBD and hACE2 was also used in this study [27].

The molecular docking simulations were performed along with the binding affinity calculations for PDB: 6M17 (SARS-CoV-2 spike protein with hACE2 receptors) and active

compounds. The interactions between active compounds and PDB: 6M17 were displayed in the best-docked poses for the calculations. These results demonstrate the high accuracy of the existing simulation system, thereby supporting further calculations. The lowest binding energy for each ligand was considered the optimal conformation, and the binding affinities are shown in Table 5. In this study, quercetin was used as a positive control. The binding energies of liquiritin (-8.2 kcal/mol), 3,5-dicaffeoylquinic acid (-8.1 kcal/mol), and luteolin-7-*O*-glucoside (-8.1 kcal/mol) were lower than those of quercetin (-7.5 kcal/mol), suggesting that these compounds can have better docking ability with the crystal structure of PDB: 6M17.

Table 5. Binding energies of active compounds and SARS-CoV-2 spike protein with human ACE2 receptors calculated in silico.

Compounds	Affinity (kcal/mol)
Chlorogenic acid	-7.8
3,5-Dicaffeoylquinic acid	-8.1
Glycyrrhizic acid	-3.5
Hesperidin	-7.7
Liquiritin	-8.2
Lobetyolin	-6.7
Luteolin-7- <i>O</i> -glucoside	-8.1
Puerarin	-7.8
Quercitrin	-7.1
Rosmarinic acid	-8.0
Quercetin ^a	-7.5

^a Quercetin was used as a positive control.

The interactions of liquiritin between SARS-CoV-2-RBD and ACE2 are shown in Figure 4. Liquiritin binds to HIS 34 of ACE2 and TYR 505 of SARS-CoV-2-RBD via conventional hydrogen bond. In addition, there are other interactions with liquiritin such as forming π -cation interactions with LYS353 and HIS34 of ACE2, π - π T-shaped interactions with TYR495 of SARS-CoV-2-RBD and HIS34 of ACE2, and π -alkyl interactions with LYS353 of ACE2, which would make stable complexes of liquiritin with SARS-CoV-2-RBD and ACE2.

The molecular docking model of 3,5-dicaffeoylquinic acid between SARS-CoV-2-RBD and receptor ACE2 is shown in Figure 5. 3,5-dicaffeoylquinic acid binds to LYS 417 and GLY 496 of SARS-CoV-2-RBD as well as ASP 30, GLN 388, and ASP 38 of ACE2 via conventional hydrogen bond. Unfavorable donor-donor interactions are found with ARG 393 of ACE2. In addition, 3,5-dicaffeoylquinic acid forms π -cation interactions with ARG 403 of SARS-CoV-2-RBD and HIS34 of ACE2, π - π T-shaped interactions with HIS34 of ACE2, and π -alkyl interactions with LYS417 of SARS-CoV-2-RBD. These interactions would allow 3,5-dicaffeoylquinic acid to form stable complexes with SARS-CoV-2-RBD and ACE2.

The interactions between luteolin-7-*O*-glucoside in SARS-CoV-2-RBD and ACE2 are shown in Figure 6. luteolin-7-*O*-glucoside binds to ASP 405 and ARG 403 of SARS-CoV-2-RBD via conventional hydrogen bond and to HIS 34 of ACE2 and ARG 403 of SARS-CoV-2-RBD via carbon-hydrogen bond. Unfavorable acceptor-acceptor interactions are found with ASN 33 of ACE2. There are other interactions with luteolin-7-*O*-glucoside, such as forming π -cation interactions with LYS353 and HIS 34 of ACE2, π -sigma interactions with HIS 34, π - π T-shaped interactions with TYR495 of SARS-CoV-2-RBD and HIS 34 of ACE2, π -alkyl interactions with LYS353 of ACE2 and ARG 403 of SARS-CoV-2-RBD, which would make stable complexes of luteolin-7-*O*-glucoside with SARS-CoV-2-RBD and ACE2.

From the above results, it can be concluded that the binding energies of liquiritin, 3,5-dicaffeoylquinic acid, and luteolin-7-*O*-glucoside are better than that of quercetin, as shown in Table 5. Likewise, the anti-SARS-CoV-2 effects of liquiritin, 3,5-dicaffeoylquinic acid, and luteolin-7-*O*-glucoside were confirmed to be superior to that of quercetin.

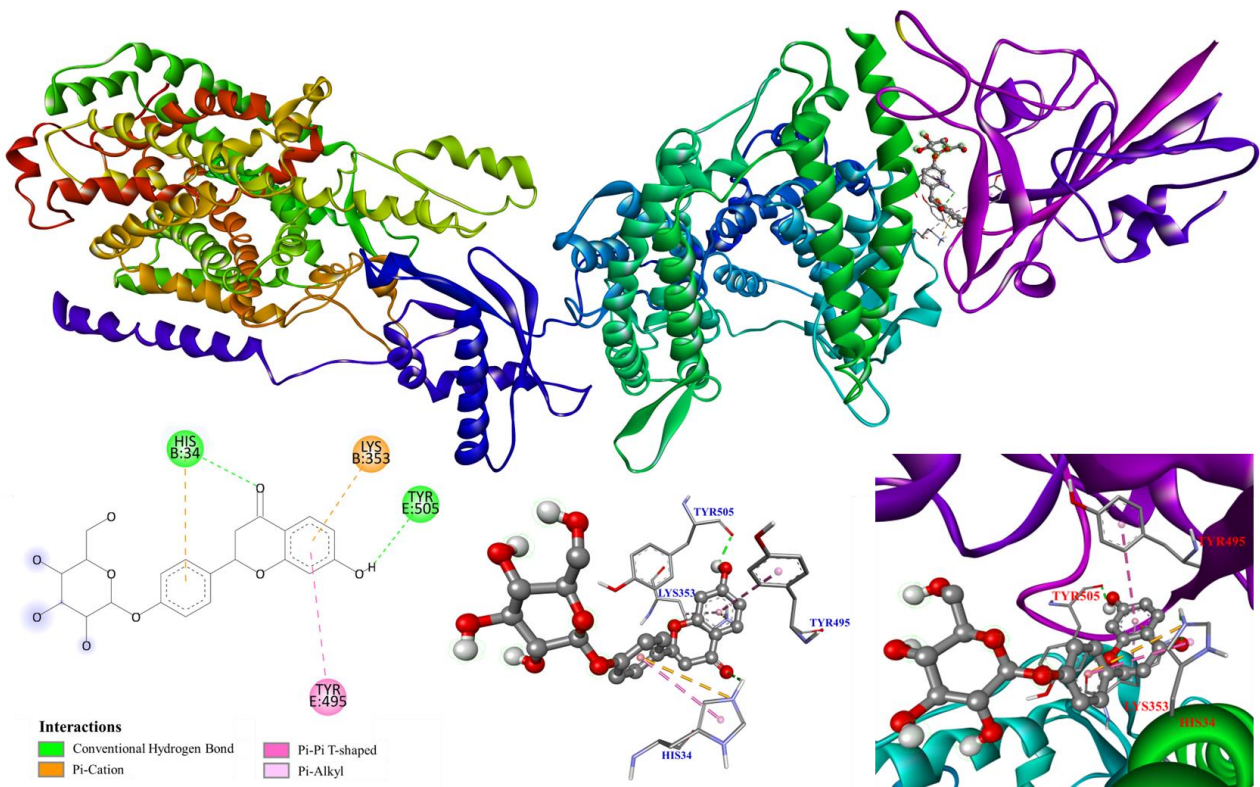


Figure 4. Interactions of liquiritin between SARS-CoV-2-RBD and ACE2 in silico.

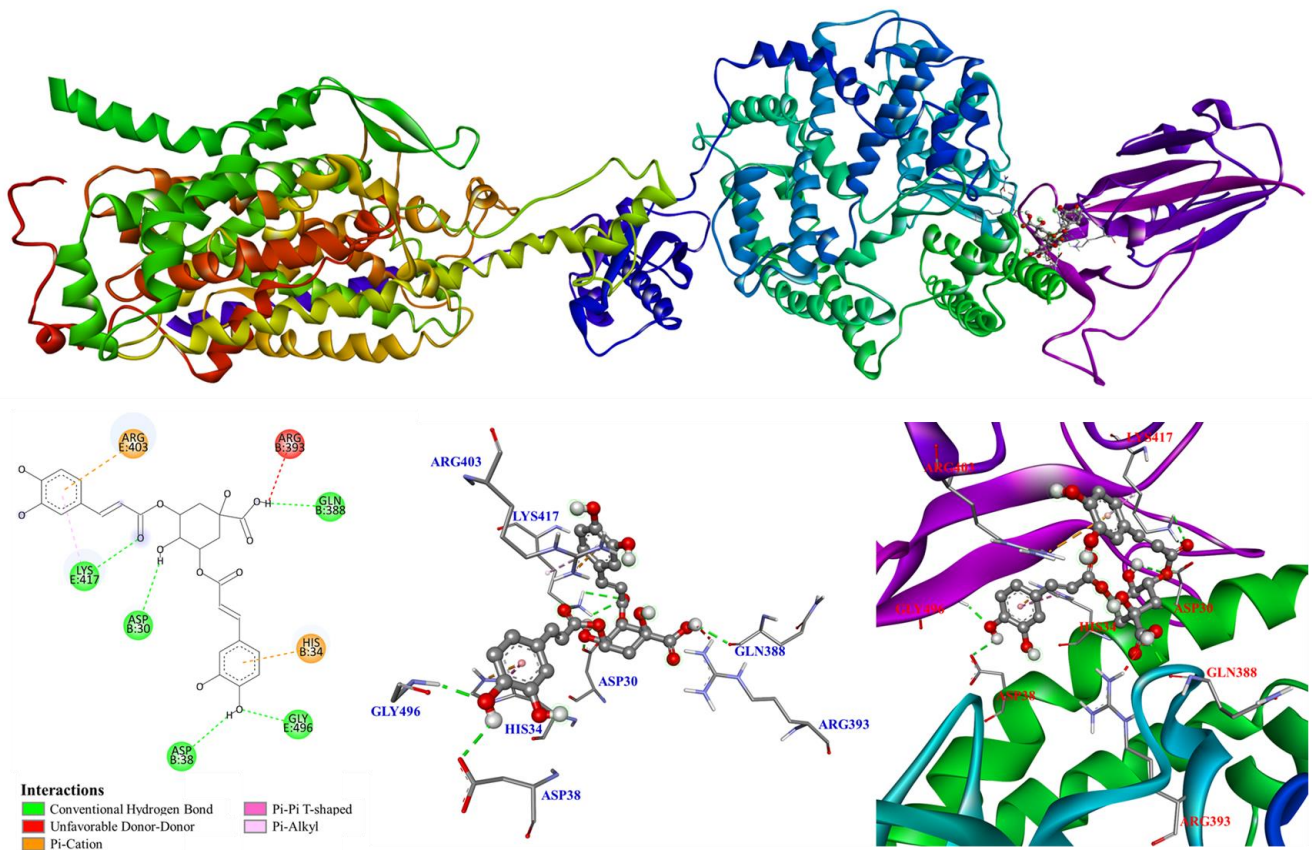


Figure 5. Interactions of 3,5-dicafeoylquinic acid between SARS-CoV-2-RBD and ACE2 in silico.

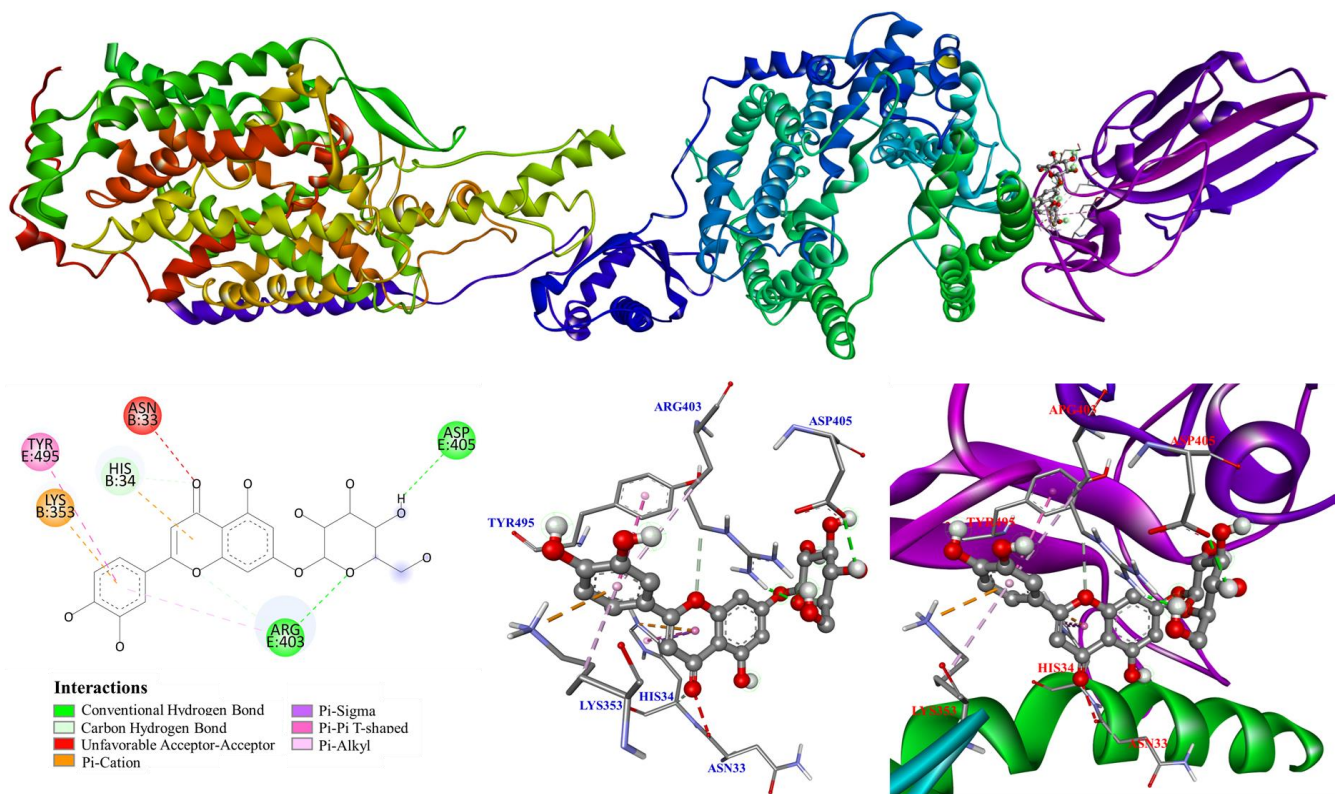


Figure 6. Interactions of luteolin-7-O-glucoside between SARS-CoV-2-RBD and ACE2 in silico.

4. Discussion

COVID-19 has caused enormous economic losses and an unprecedented health crisis across the globe. How to provide prevention and treatment are important in disease management. The SARS-CoV-2 vaccine has been developed. It has been shown to reduce the risk of deaths and serious illness from COVID-19. Moreover, recent reports indicate that adverse drug reactions of the SARS-CoV-2 vaccine are a critical issue, and SARS-CoV-2 variants may increase the risk of breakthrough infection and reduce vaccine efficiency for protective immunity [28–30]. Therefore, developing different strategies to prevent COVID-19 is a critical priority.

TCM formula has been composed of different herbs, the active components of which can target various pathways. Herbs are widely used as a preventive method for many infections and diseases due to their ability to anti-viruses and modulate the immune system [31,32]. Lianhua Qingwen Capsules, Qingfei Paidu Decoction, and Shufeng Jiedu Capsules are commonly used in TCM for the treatment of COVID-19 [33]. The literature of Yueh-Hsin Ping shows Jing Guan Fang can prevent SARS-CoV-2 infection, including inhibition of syncytia formation and inhibition of viral plaque formation [10]. TCM formula of NRICM101 may disrupt disease progression by its against SARS-CoV-2 infection and anti-inflammatory activity [9]. Previous studies have shown that the spike protein is key for SARS-CoV-2 to infect host cells. Some crucial residues of S-protein can physically interact with human receptor ACE2 to prime infection and may as a target against SARS-CoV-2 infection. Amino acids involved in protein-protein interactions of Human ACE2 and SARS-CoV-2 spike protein, including Ser438, Gly476, Asn479, and Val48 residues of the S protein, as well as Lys26, Thr27, Glu37, Lys68, Asp206, Gly211, Arg219, Gly326, Lys341, Gly352, Asp355, Pro389, Val447, Ile468 and the Arg559 residue of ACE2 [34]. In addition, many compounds exhibit molecular docking affinity for SARS-CoV-2 replicase, such as 3,5-dicaffeoylquinic acid, liquiritin, astragaloside IV, and luteolin-7-O-glucoside [35–38]. Our data show that PAFYY displays anti-SARS-CoV-2 activity and is rich in quercitrin, rosmarinic acid, hesperidin, chlorogenic acid, liquiritin, 3,5-dicaffeoylquinic acid, lobety-

olin, astragaloside IV, puerarin, glycyrrhizic acid, luteolin-7-*O*-glucoside. The interaction between SARS-CoV-2 and ACE2 may be related to *Houttuynia*, *Mentha*, *Codonopsis*, *Platycodon grandiflorum*, and *Perilla* leaves in PAFYY. Further molecular docking computing results support that the binding affinity of liquiritin, 3,5-dicaffeoylquinic acid, and luteolin-7-*O*-glucoside between SARS-CoV-2-RBD and hACE2 receptor is significantly higher than other compounds and the positive control quercetin.

The oxidant stress and inflammation are related to pathophysiological processes of respiratory viral diseases. Overproduction of reactive oxygen species (ROS) and disturbances of antioxidant defenses have been associated with virus-mediated disease, including cytokine storms and severe inflammation. Nrf2 and NF- κ B are crucial molecules on oxidative stress and inflammation pathway, respectively. A recent report demonstrated that SARS-CoV-2 infection could inhibit Nrf2 and activate NF- κ B pathways, then leading to inflammation and oxidative damage. Antioxidants can scavenge reactive oxygen species and inhibit oxidant-producing enzymes. SOD can reduce free radical storms that occur in viral infections [39,40]. SARS-CoV-2 infection stimulates the arachidonic acid cascade through the lipoxygenase pathway, and the 5-LOX pathway is implicated in viral pathophysiology [7]. In this study, PAFYY can protect the host from oxidative and inflammatory stress damage caused by COVID-19. The free radical scavenging activity of PAFYY may be related to *Pueraria*, *Honeysuckle* flower, *Mentha*, and *Perilla* leaf. *Houttuynia*, *Astragalus*, *Citrus Peel*, *Agastache*, and *Platycodon* provide SOD activity of PAFYY, and the *Houttuynia*, *Mentha*, and *Honeysuckle* flower provide LOX inhibition of PAFYY.

It is well known that the composition of Chinese herbal medicine is complex. TCM formulations need to be standardized in terms of safety, efficacy, and potency. Quality control of medicinal materials requires the use of a variety of techniques, including HPLC, ICP-MS, LC-MS, and GC-MS are used for the quantitative estimation and quality control assessment [22,41,42]. Our data show that a total of eleven representative constituents were quantitative analyses performed by HPLC/PDA or ELSD method, saccharide compositions were quantitatively determined by HPLC/ELSD or HPLC/RI, twenty amino acids were quantitatively determined by LC-MS/MS, and trace elements were semiquantitative analysis by ICP/MS in PAFYY. The content of heavy metals in PAFYY is lower than the limit specified, and our data provide information on the safety of medicinal materials (Supplementary Table S3). In addition, the chemical composition of PAFYY may depend on how it is brewed. Our study also describes the chemical composition of PAFYY prepared with different brewing times. In Supplementary Table S4, the contents of most components increased gradually in a while. More than 50% of phytochemicals can be dissolved in boiling water for 30 min of steep time. Thus, a variety of chromatographic techniques have been successfully applied to analyze PAFYY, and it provides a reference and useful method for the quality control of PAFYY in the future.

5. Conclusions

To our knowledge, this study is the first to investigate the chemical composition of PAFYY and its potential to prevent SARS-CoV-2 infection. As mentioned above, PAFYY may be involved in a variety of mechanisms, which may prevent or improve COVID-19 syndrome. Molecular docking calculations supported the binding affinity of PAFYY's biologically active compounds between SARS-CoV-2-RBD and the hACE2 receptor. Chemical fingerprint data provide comprehensive information for PAFYY's quality control in the future. Moreover, the potential of PAFYY to prevent COVID-19 requires further validation *in vivo*, including benefits for COVID-19 and pharmacokinetic description.

Supplementary Materials: The following supporting information can be downloaded at: <https://www.mdpi.com/article/10.3390/pr10112213/s1>, Figure S1: Chromatographic profile of reference standards (A) and PAFYY (B) from HPLC/ELSD. Figure S2: Chromatographic profile of polysaccharide (A), stachyose (B) fructose, glucose and sucrose (C) in PAFYY. Table S1: Amino acids in PAFYY. Table S2: The content of trace elements in PAFYY. Table S3: The heavy metal content of PAFYY. Table S4: Chemical composition changes of PAFYY at different times.

Author Contributions: Y.-C.T. performed the bioassay and manuscript writing. Y.-H.H. conducted molecular docking and manuscript writing. C.-Y.C. and K.-T.W. analyzed the quantification of components. J.-J.C., Y.-C.T., M.-C.L. and W.-C.C. planned, designed, and organized all the research for this study and the preparation of the manuscript. All authors have read and agreed to the published version of the manuscript.

Funding: This research was supported by a grant from the Ministry of Science and Technology (MOST), Taiwan (No. MOST 109-2320-B-010-029-MY3), awarded to J.-J. Chen.

Institutional Review Board Statement: Not applicable.

Informed Consent Statement: Not applicable.

Data Availability Statement: The data is confidential.

Conflicts of Interest: The authors declare no conflict of interest.

References

1. World Health Organization. WHO Coronavirus (COVID-19) Dashboard. Available online: <https://covid19.who.int/> (accessed on 7 September 2022).
2. World Health Organization. Coronavirus Disease (COVID-19). Available online: https://www.who.int/health-topics/coronavirus#tab=tab_1 (accessed on 6 June 2022).
3. Zhu, N.; Zhang, D.; Wang, W.; Li, X.; Yang, B.; Song, J.; Zhao, X.; Huang, B.; Shi, W.; Lu, R.; et al. A novel coronavirus from patients with pneumonia in China. *N. Engl. J. Med.* **2019**, *382*, 727–733. [[CrossRef](#)] [[PubMed](#)]
4. Huang, Y.; Yang, C.; Xu, X.F.; Xu, W.; Liu, S.W. Structural and functional properties of SARS-CoV-2 spike protein: Potential antiviral drug development for COVID-19. *Acta. Pharmacol. Sin.* **2020**, *41*, 1141–1149. [[CrossRef](#)] [[PubMed](#)]
5. Li, Q.; Wang, Y.; Sun, Q.; Knopf, J.; Herrmann, M.; Lin, L.; Jiang, J.; Shao, C.; Li, P.; He, X.; et al. Immune response in COVID-19: What is next? *Cell Death Differ.* **2022**, *29*, 1107–1122. [[CrossRef](#)] [[PubMed](#)]
6. Ripon, M.A.R.; Bhowmik, D.R.; Amin, M.T.; Hossain, M.S. Role of arachidonic cascade in COVID-19 infection: A review. *Prostaglandins Other Lipid Mediat.* **2021**, *154*, 106539. [[CrossRef](#)] [[PubMed](#)]
7. Ayola-Serrano, N.C.; Roy, N.; Fathah, Z.; Anwar, M.M.; Singh, B.; Ammar, N.; Sah, R.; Elba, A.; Utt, R.S.; Pecho-Silva, S.; et al. The role of 5-lipoxygenase in the pathophysiology of COVID-19 and its therapeutic implications. *Inflamm. Res.* **2021**, *70*, 877–889. [[CrossRef](#)]
8. DE Flora, S.; Balansky, R.; LA Maestra, S. Antioxidants and COVID-19. *J. Prev. Med. Hyg.* **2021**, *62* (Suppl. S3), 34–45.
9. Tsai, C.I.; Chiou, C.T.; Lin, C.J.; Wei, W.C.; Lin, S.J.; Tseng, Y.H.; Yeh, K.M.; Lin, Y.L.; Jan, J.T.; Liang, J.J.; et al. A traditional Chinese medicine formula NRICM101 to target COVID-19 through multiple pathways: A bedside-to-bench study. *Biomed. Pharmacother.* **2021**, *133*, 111037. [[CrossRef](#)]
10. Ping, Y.H.; Yeh, H.; Chu, L.W.; Lin, Z.H.; Hsu, Y.C.; Lin, L.C.; Hsu, C.H.; Fu, S.L.; Lin, T.Y. The traditional Chinese medicine formula Jing Guan Fang for preventing SARS-CoV-2 infection: From clinical observation to basic research. *Front. Pharmacol.* **2022**, *13*, 744439. [[CrossRef](#)]
11. Zhao, Z.; Li, Y.; Zhou, L.; Zhou, X.; Xie, B.; Zhang, W.; Sun, J. Prevention and treatment of COVID-19 using traditional Chinese medicine: A review. *Phytomedicine* **2021**, *85*, 153308. [[CrossRef](#)]
12. Li, B.H.; Li, Z.Y.; Liu, M.M.; Tian, J.Z.; Cui, Q.H. Progress in traditional Chinese medicine against respiratory viruses: A review. *Front. Pharmacol.* **2021**, *12*, 743623. [[CrossRef](#)]
13. Yang, Y.; Islam, M.S.; Wang, J.; Li, Y.; Chen, X. Traditional Chinese medicine in the treatment of patients infected with 2019-new coronavirus (SARS-CoV-2): A review and perspective. *Int. J. Biol. Sci.* **2020**, *16*, 1708–1717. [[CrossRef](#)] [[PubMed](#)]
14. Lyu, M.; Fan, G.; Xiao, G.; Wang, T.; Xu, D.; Gao, J.; Ge, S.; Li, Q.; Ma, Y.; Zhang, H.; et al. Traditional Chinese medicine in COVID-19. *Acta. Pharm. Sin. B* **2021**, *11*, 3337–3363. [[CrossRef](#)] [[PubMed](#)]
15. Pan, B.; Fang, S.; Zhang, J.; Pan, Y.; Liu, H.; Wang, Y.; Li, M.; Liu, L. Chinese herbal compounds against SARS-CoV-2: Puerarin and quercetin impair the binding of viral S-protein to ACE2 receptor. *Comput. Struct. Biotechnol. J.* **2020**, *18*, 3518–3527. [[CrossRef](#)]
16. Serlahwaty, D.; Giovani, C. In silico screening of mint leaves compound (*Mentha piperita* L.) as a potential inhibitor of SARS-CoV-2. *Pharm. Educ.* **2021**, *21*, 81–86.
17. Tang, W.F.; Tsai, H.P.; Chang, Y.H.; Chang, T.Y.; Hsieh, C.F.; Lin, C.Y.; Lin, G.H.; Chen, Y.L.; Jheng, J.R.; Liu, P.C.; et al. Perilla (*Perilla frutescens*) leaf extract inhibits SARS-CoV-2 via direct virus inactivation. *Biomed. J.* **2021**, *44*, 293–303. [[CrossRef](#)] [[PubMed](#)]
18. Huang, J.; Tao, G.; Liu, J.; Cai, J.; Huang, Z.; Chen, J. Current Prevention of COVID-19: Natural products and herbal medicine. *Front. Pharmacol.* **2022**, *11*, 588508. [[CrossRef](#)] [[PubMed](#)]
19. Huang, W.M.; Liang, Y.Q.; Tang, L.J.; Ding, Y.; Wang, X.H. Antioxidant and anti-inflammatory effects of Astragalus polysaccharide on EA.hy926 cells. *Exp. Ther. Med.* **2013**, *6*, 199–203. [[CrossRef](#)]
20. Prieto, J.M.; Schinella, G.R. Anti-inflammatory and antioxidant Chinese herbal medicines: Links between traditional characters and the skin lipoperoxidation “Western” model. *Antioxidants* **2022**, *11*, 611. [[CrossRef](#)]

21. Wang, S.; Wang, J.; Yu, X.; Jiang, W.; Chen, S.; Wang, R.; Wang, M.; Jiao, S.; Yang, Y.; Wang, W.; et al. Antibody-dependent enhancement of SARS-CoV-2 pseudoviral infection requires FcγRIIB and virus-antibody complex with bivalent interaction. *Commun. Biol.* **2022**, *5*, 262. [[CrossRef](#)]
22. Lin, I.H.; Lee, M.C.; Chuang, W.C. Application of LC/MS and ICP/MS for establishing the fingerprint spectrum of the traditional Chinese medicinal preparation Gan-Lu-Yin. *J. Sep. Sci.* **2006**, *29*, 172–179. [[CrossRef](#)]
23. Trott, O.; Olson, A.J. AutoDock Vina: Improving the speed and accuracy of docking with a new scoring function, efficient optimization, and multithreading. *J. Comput. Chem.* **2010**, *31*, 455–461. [[CrossRef](#)] [[PubMed](#)]
24. *BIOVIA Discovery Studio Client 2021*, v.21.1.0; Dassault Systèmes: San Diego, CA, USA, 2021.
25. Chen, Q.; Wang, D.; Tan, C.; Hu, Y.; Sundararajan, B.; Zhou, Z. Profiling of flavonoid and antioxidant activity of fruit tissues from 27 Chinese local citrus cultivars. *Plants* **2020**, *9*, 196. [[CrossRef](#)] [[PubMed](#)]
26. Hsu, H.F.; Hsiao, P.C.; Kuo, T.C.; Chiang, S.T.; Chen, S.L.; Chiou, S.J.; Ling, X.H.; Liang, M.T.; Cheng, W.Y.; Hough, J.Y. Antioxidant and anti-inflammatory activities of *Lonicera japonica* Thunb. var. *sempervillosa* Hayata flower bud extracts prepared by water, ethanol, and supercritical fluid extraction techniques. *Ind. Crops Prod.* **2016**, *89*, 543–549. [[CrossRef](#)] [[PubMed](#)]
27. Yan, R.; Zhang, Y.; Li, Y.; Xia, L.; Guo, Y.; Zhou, Q. Structural basis for the recognition of SARS-CoV-2 by full-length human ACE2. *Science* **2020**, *367*, 1444–1448. [[CrossRef](#)] [[PubMed](#)]
28. Hu, J.; Peng, P.; Cao, X.; Wu, K.; Chen, J.; Wang, K.; Tang, N.; Huang, A.L. Increased immune escape of the new SARS-CoV-2 variant of concern Omicron. *Cell Mol. Immunol.* **2022**, *19*, 293–295. [[CrossRef](#)] [[PubMed](#)]
29. Tregoning, J.S.; Flight, K.E.; Higham, S.L.; Wang, Z.; Pierce, B.F. Progress of the COVID-19 vaccine effort: Viruses, vaccines and variants versus efficacy, effectiveness and escape. *Nat. Rev. Immunol.* **2021**, *21*, 626–636. [[CrossRef](#)] [[PubMed](#)]
30. Gasmı, A.; Chirumbolo, S.; Peana, M.; Noor, S.; Menzel, A.; Dadar, M.; Bjørklund, G. The role of diet and supplementation of natural products in COVID-19 prevention. *Biol. Trace Elem. Res.* **2022**, *200*, 27–30. [[CrossRef](#)] [[PubMed](#)]
31. Al-Doori, A.; Ahmed, D.; Kadhom, M.; Yousif, E. Herbal medicine as an alternative method to treat and prevent COVID-19. *Baghdad. J. Biochem. Appl. Biol. Sci.* **2021**, *2*, 1–20. [[CrossRef](#)]
32. Rathinavel, T.; Meganathan, B.; Kumarasamy, S.; Ammashi, S.; Thangaswamy, S.; Ragunathan, Y.; Palanisamy, S. Potential COVID-19 drug from natural phenolic compounds through in silico virtual screening approach. *Biointerface Res. Appl. Chem.* **2021**, *11*, 10161–10173.
33. Kang, X.; Jin, D.; Jiang, L.; Zhang, Y.; Zhang, Y.; An, X.; Duan, L.; Yang, C.; Zhou, R.; Duan, Y.; et al. Efficacy and mechanisms of traditional Chinese medicine for COVID-19: A systematic review. *Chin. Med.* **2022**, *17*, 30. [[CrossRef](#)]
34. Senapati, S.; Banerjee, P.; Bhagavatula, S.; Kushwaha, P.P.; Kumar, S. Contributions of human ACE2 and TMPRSS2 in determining host-pathogen interaction of COVID-19. *J. Genet.* **2021**, *100*, 12. [[CrossRef](#)] [[PubMed](#)]
35. Wu, H.; Gong, K.; Qin, Y.; Yuan, Z.; Xia, S.; Zhang, S.; Yang, J.; Yang, P.; Li, L.; Xie, M. In silico analysis of the potential mechanism of a preventive Chinese medicine formula on coronavirus disease 2019. *J. Ethnopharmacol.* **2021**, *275*, 114098. [[CrossRef](#)] [[PubMed](#)]
36. Shah, S.; Chaple, D.; Arora, S.; Yende, S.; Mehta, C.; Nayak, U. Prospecting for *Cressa cretica* to treat COVID-19 via in silico molecular docking models of the SARS-CoV-2. *J. Biomol. Struct. Dyn.* **2021**, *40*, 5643–5652. [[CrossRef](#)] [[PubMed](#)]
37. Ahmed, B.; Abdalla, M.; Sharaf, M.; Al-Resayes, S.; Imededdine, K.; Mahboob, A.; Yagi, S.; Azam, M.; Yousfi, M. In-silico investigation of phenolic compounds from leaves of *Phillyrea angustifolia* L. as a potential inhibitor against the SARS-CoV-2 main protease (M^{Pro} PDB ID:5R83) using a virtual screening method. *J. Saudi Chem. Soc.* **2022**, *26*, 101473.
38. Mbikay, M.; Chrétien, M. Isoquercetin as an anti-COVID-19 medication: A potential to realize. *Front. Pharmacol.* **2022**, *13*, 830205. [[CrossRef](#)]
39. Mrityunjaya, M.; Pavithra, V.; Neelam, R.; Janhavi, P.; Halami, P.M.; Ravindra, P.V. Immune-boosting, antioxidant and anti-inflammatory food supplements targeting pathogenesis of COVID-19. *Front. Immunol.* **2022**, *11*, 570122. [[CrossRef](#)]
40. Wu, J. Tackle the free radicals damage in COVID-19. *Nitric Oxide.* **2020**, *102*, 39–41. [[CrossRef](#)]
41. Luo, L.; Wang, B.; Jiang, J.; Fitzgerald, M.; Huang, Q.; Yu, Z.; Li, H.; Zhang, J.; Wei, J.; Yang, C.; et al. Heavy Metal Contaminations in Herbal Medicines: Determination, Comprehensive Risk Assessments, and Solutions. *Front. Pharmacol.* **2021**, *11*, 595335. [[CrossRef](#)]
42. Balekundri, A.; Mannur, V. Quality control of the traditional herbs and herbal products: A review. *Futur. J. Pharm. Sci.* **2020**, *6*, 67. [[CrossRef](#)]